Solution Properties of Perfluorinated Anionic Surfactants with Divalent Counterion of Separate Electric Charges

ARTICLE *in* LANGMUIR · SEPTEMBER 2007

Impact Factor: 4.46 · DOI: 10.1021/la7005474 · Source: PubMed

5 AUTHORS, INCLUDING:

Hiromichi Nakahara
Nagasaki International University
47 PUBLICATIONS **585** CITATIONS
SEE PROFILE

Satoru Karasawa
Kyushu University
60 PUBLICATIONS **975** CITATIONS
SEE PROFILE

Yoshikiyo Moroi
Nagasaki International University
146 PUBLICATIONS **2,764** CITATIONS
SEE PROFILE

Osamu Shibata
Nagasaki International University
102 PUBLICATIONS **1,500** CITATIONS
SEE PROFILE

Solution Properties of Perfluorinated Anionic Surfactants with Divalent Counterion of Separate Electric Charges

Jyunya Masuda,[†] Hiromichi Nakahara,[†] Satoru Karasawa,[§] Yoshikiyo Moroi,[†] and Osamu Shibata*[,†,‡]

Division of Biointerfacial Science, and Department of Chemo-Pharmaceutical Sciences, Graduate School of Pharmaceutical Sciences, Kyushu University, 3-1-1 Maidashi, Higashi-ku, Fukuoka 812-8582, Japan, and Department of Biophysical Chemistry, Faculty of Pharmaceutical Sciences, Nagasaki International University, 2825-7 Huis Ten Bosch, Sasebo, Nagasaki 859-3298, Japan

Received February 24, 2007. In Final Form: May 21, 2007

Novel surfactants of perfluorinated double long-chain salts with divalent counterion of separate electric charge, 1,1-(1,ω-alkanediyl)bispyridinium diperfluorononanoate ($C_nBP(FC_9)_2$, $n = 2, 4, 6, 8$) were newly synthesized. Their solution properties were investigated by surface tension measurement over the temperature range from 298.2 to 313.2 K, where magnesium diperfluorononanoate ($Mg(FC_9)_2$) was employed as a reference surfactant with divalent counterion of concentrated electric charge. From change of surface tension with concentration, the critical micelle concentration (CMC), surface excess (Γ), apparent molecular surface area (A), and $-\log$(concentration to reduce surface tension of water by 20 mN m^{-1}) (pC_{20}) were determined. The CMC values of $C_nBP(FC_9)_2$ decreased with increasing charge separation and with increasing temperature, where the values of $C_nBP(FC_9)_2$ were much smaller than those of $Mg(FC_9)_2$. In addition, the pC_{20} values of the former were also much larger than those of the latter. These results indicate a strong influence of the extent of charge separation or the spacer length of the counterions upon surface activity of the fluorinated surfactants. The surface excess or the corresponding apparent molecular surface area monotonously changed with the spacer length ($n \leq 6$), whereas the behavior for $n = 8$ was much different from the other $C_nBP(FC_9)_2$ due to conformational change in the in-between alkanediyl chain. The entropy changes (Δs) for the surface adsorption or condensation were found to be mostly negative for $C_nBP(FC_9)_2$, where the changes approached zero with an increase in the charge separation. On the other hand, the changes for $Mg(FC_9)_2$ were positive over the whole concentration below the CMC. In addition, Brewster angle microscopy indicated no condensation of the present surfactants just at the air/solution interface.

Introduction

Fluorine is the most electronegative of all elements, although it is very small in size. It is well-known that replacing the hydrogen atoms by fluorine atoms causes dramatic change in the physicochemical properties of chemical compounds. Fluorinated surfactants, for example, exhibit considerable thermal stability, chemical stability, high gas-dissolving capacity, hydrophobicity, lipophobicity, and excellent activity such as a remarkably low critical micelle concentration (CMC), availability even in organic solvent, and high efficiency in reducing surface tension.[1,2] These properties are characterized by strong intramolecular bonds (C−F bond) and weak intermolecular interactions between fluorocarbons, which brings about such various applications of fluorinated surfactants as emulsifier, detergent, additive in inks or drugs, dental use, blood substitute, and so on.[3−7]

Solution properties of ionic surfactants are strongly influenced by chemical species of counterions. Counterions of conventional anionic surfactants are usually alkali or alkaline earth metal ions whose electric charges are concentrated within the size of the ions. In the previous study, anionic surfactants with nonmetallic divalent cationic counterions whose electric charge is not concentrated but diffused or separated were found to have quite different physicochemical properties from those of usually hydrogenated ones.[8,9] In particular, the properties of anionic surfactants with charge-separated counterions, 1,1′-(1,ω-alkanediyl)bispyridinium tetradecane sulfonates ($C_nBP(HC_{14})_2$), depended much on the extent of charge separation of the divalent counterion.[10,11]

In the present study, anionic perfluorinated surfactants with various charge-separated divalent counterions, 1,1′-(1,ω-alkanediyl)bispyridinium diperfluorononanoate (($C_nBP(FC_9)_2$, $n = 2, 4, 6, 8$) were newly synthesized and then investigated in order to clarify their solution properties and to examine the effect of the extent of charge separation. Furthermore, the results were compared with those of the same surfactant ions with concentrated divalent counterion (Mg^{2+}) and monovalent counterion (Li^+, Na^+, K^+, and NH_4^+)[12] and with those of corresponding

* Corresponding author. Osamu Shibata, Department of Biophysical Chemistry, Faculty of Pharmaceutical Sciences, Nagasaki International University, 2825-7 Huis Ten Bosch, Sasebo, Nagasaki 859-3298, Japan. E-mail: wosamu@niu.ac.jp.

[†] Division of Biointerfacial Science, Kyushu University.

[‡] Nagasaki International University.

[§] Department of Chemo-Pharmaceutical Sciences, Kyushu University.

(1) Shinoda, K.; Hato, M.; Hayashi, T. *J. Phys. Chem.* **1972**, *76*, 909−914.
(2) Krafft, M. P.; Riess, J. G. *Biochimie* **1998**, *80*, 489−514.
(3) Riess, J. G.; Krafft, M. P. *Biomaterials* **1998**, *19*, 1529−1539.
(4) Riess, J. G. *Chem. Rev.* **2001**, *101*, 2797−2920.
(5) Dias, A. M. A.; Freire, M.; Coutinho, J. A. P.; Marrucho, I. M. *Fluid Phase Equilib.* **2004**, *222*−*223*, 325−330.
(6) Freire, M. G.; Dias, A. M. A.; Coelho, M. A. Z.; Coutinho, J. A. P.; Marrucho, I. M. *J. Colloid Interface Sci.* **2005**, *286*, 224−232.
(7) Freire, M. G.; Gomes, L.; Santos, L. M. N. B. F.; Marrucho, I. M.; Coutinho, J. A. P. *J. Phys. Chem. B* **2006**, *110*, 22923−22929.
(8) Moroi, Y.; Ikeda, N.; Matuura, R. *J. Colloid Interface Sci.* **1984**, *101*, 285−288.
(9) Moroi, Y.; Sugii, R.; Akine, C.; Matuura, R. *J. Colloid Interface Sci.* **1985**, *108*, 180−188.
(10) Moroi, Y.; Matuura, R.; Kuwamura, T.; Inokuma, S. *J. Colloid Interface Sci.* **1986**, *113*, 225−231.
(11) Moroi, Y.; Matuura, R.; Tanaka, M.; Murata, Y.; Aikawa, Y.; Furutani, E.; Kuwamura, T.; Takahashi, H.; Inokuma, S. *J. Phys. Chem.* **1990**, *94*, 842−845.
(12) Kunieda, H.; Shinoda, K. *J. Phys. Chem.* **1976**, *80*, 2468−2470.

10.1021/la7005474 CCC: $37.00
Published on Web 07/18/2007

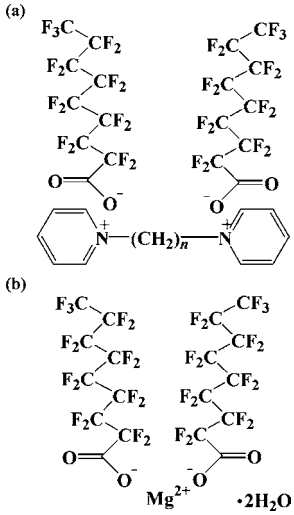

Figure 1. Chemical structures of (a) $C_nBP(FC_9)_2$, $n = 2, 4, 6, 8$; and (b) $Mg(FC_9)_2 \cdot 2H_2O$.

Table 1. Elemental Analysis of $C_nBP(FC_9)_2$ and $Mg(FC_9)_2 \cdot 2H_2O$

compound		C (%)	H (%)	N (%)
$C_2BP(FC_9)_2$	calc.	32.39	1.27	2.52
	found	32.29	1.26	2.59
$C_4BP(FC_9)_2$	calc.	33.70	1.59	2.46
	found	33.91	1.92	2.85
$C_6BP(FC_9)_2$	calc.	34.94	1.90	2.40
	found	34.95	2.05	2.55
$C_8BP(FC_9)_2$	calc.	36.13	2.19	2.34
	found	35.99	2.29	2.52
$Mg(FC_9)_2 \cdot 2H_2O$	calc.	21.92	0.41	
	found	22.01	0.46	

tetradecane sulfonates $C_nBP(HC_{14})_2$.[10,11] The interfacial behavior of $C_nBP(FC_9)_2$ was also morphologically examined by Brewster angle microscopy.

Experimental Section

Materials. 1,1′-(1,ω-Alkanediyl)bispyridinium perfluorononanoates (abbr. $C_n(FC_9)_2$; $n = 2, 4, 6, 8$) were synthesized by complex decomposition of 1,1′-(1,ω-alkanediyl)bispyridinium bromide with silver perfluorononanoate (Figure 1). The former was the gift from the former Kuwamura laboratory of Gunma University which were the same as used in the previous study.[10] On the other hand, the latter was prepared by neutralization of perfluorononanoic acid (Daikin Industries, Ltd., >95.0%) by lithium hydroxide (Kanto Chemical Co., Inc., 99.0%) in water and by followed conversion of the lithium salt to the silver salt with silver nitrate (nacalai tesque, 99.9%). The exchange of the silver ion by the bispyridinium ion was carried out as reported previously.[10] Magnesium diperfluorononanoate (abbr. $Mg(FC_9)_2$) was also synthesized by neutralization of magnesium hydroxide (Wako chemical, 99.0%) by perfluorononanoic acid (Figure 1). The obtained crude crystals of $C_nBP(FC_9)_2$ were purified by thrice recrystallizations from ethanol (for $n = 2, 4, 6$) and from acetone/ethanol (3/1, v/v) (for $n = 8$), while ethanol/methanol (2/1, v/v) was used for $Mg(FC_9)_2$. Their purities were checked by elemental analysis (Table 1). From the analyses, only $Mg(FC_9)_2$ was found to have two water molecules of crystallization, $Mg(FC_9)_2 \cdot 2H_2O$. In addition, a representative of their three-dimensional structures in the crystalline state was obtained by X-ray structure analysis (Rigaku Raxis-Rapid diffractometer, Rigaku Corp., Japan) with graphite monochromated Mo Kα radiation ($\lambda = 0.210\ 69$ Å) (Figure 2). The water used throughout the syntheses and measurements was thrice-distilled one (surface tension = 71.99 mN m^{-1} at 298.2 K and electrical resistivity = 18 MΩ cm).

Surface Tension Measurement. The surface tension (γ) of the surfactant solutions was determined over the temperature range 298.2−313.2 K with every 5 K interval using a drop volume tensiometer (DVS-2000, YTS, Japan). This tensiometer measures the volume of a drop detaching from a capillary with known diameter. The temperature was kept constant within ±0.03 K by means of a thermostat.[13] The experimental error for estimating the surface tension was ±0.05 mN m^{-1}.

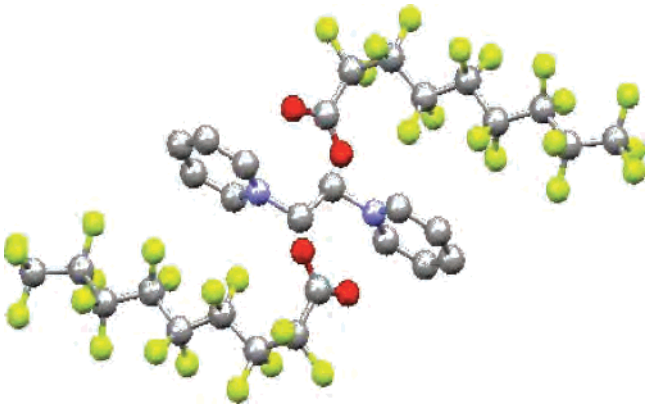

Figure 2. The crystal structure of $C_2BP(FC_9)_2$ by X-ray analysis.

Table 2. The CMC and Surface Tension Above the CMC (γ_{eq}) of Each Compound at Different Temperatures

compound	temp. (K)	CMC (mM)	γ_{eq} (mN m^{-1})
$C_2BP(FC_9)_2$	298.2	0.31	16.14
	303.2	0.34	15.92
	308.2	0.32	15.68
	313.2	0.37	15.38
$C_4BP(FC_9)_2$	298.2	0.28	18.05
	303.2	0.30	17.70
	308.2	0.30	17.51
	313.2	0.32	17.22
$C_6BP(FC_9)_2$	298.2	0.23	20.12
	303.2	0.25	19.63
	308.2	0.26	19.51
	313.2	0.29	19.16
$C_8BP(FC_9)_2$	298.2	0.16	21.15
	303.2	0.17	21.11
	308.2	0.18	20.58
	313.2	0.19	20.56
$Mg(FC_9)_2$	298.2	1.65	17.71
	303.2	1.64	17.63
	308.2	1.62	17.30
	313.2	1.59	17.14
$C_2BP(HC_{14})_2$[a]	308.2	0.19	–
$C_4BP(HC_{14})_2$[a]		0.20	–
$C_6BP(HC_{14})_2$[a]		0.19	–
$C_8BP(HC_{14})_2$[a]		0.14	–
$C_8F_{17}COOLi$[b]	298.2	10.6 (303.2K)	24.6
$C_8F_{17}COONa$[b]		9.1 (303.2K)	21.5
$C_8F_{17}COOK$[b]		6.3 (323.2K)	20.6
$C_8F_{17}COONH_4$[b]		6.7 (303.2K)	14.8

[a] Refs 10 and 11. [b] Ref 12.

Brewster Angle Microscopy (BAM). The morphology of $C_nBP(FC_9)_2$ solutions near the air/water interface was directly visualized by a Brewster angle microscope (KSV Optrel BAM 300, KSV Instruments Ltd., Finland) at 298.2 ± 0.3 K. The application of a 20 mW He−Ne laser and 10× objective allowed a lateral resolution of ca. 2 μm. The angle of the incident beam to the air−water interface was fixed to the Brewster angle (53.1°). The reflected beam was recorded with a high-grade CCD camera (EHDkamPro02, EHD imaging GmbH, Germany), and then the BAM images were digitally saved to the computer hard disk.

(13) Rusdi, M.; Moroi, Y.; Nakahara, H.; Shibata, O. *Langmuir* **2005**, *21*, 7308−7310.

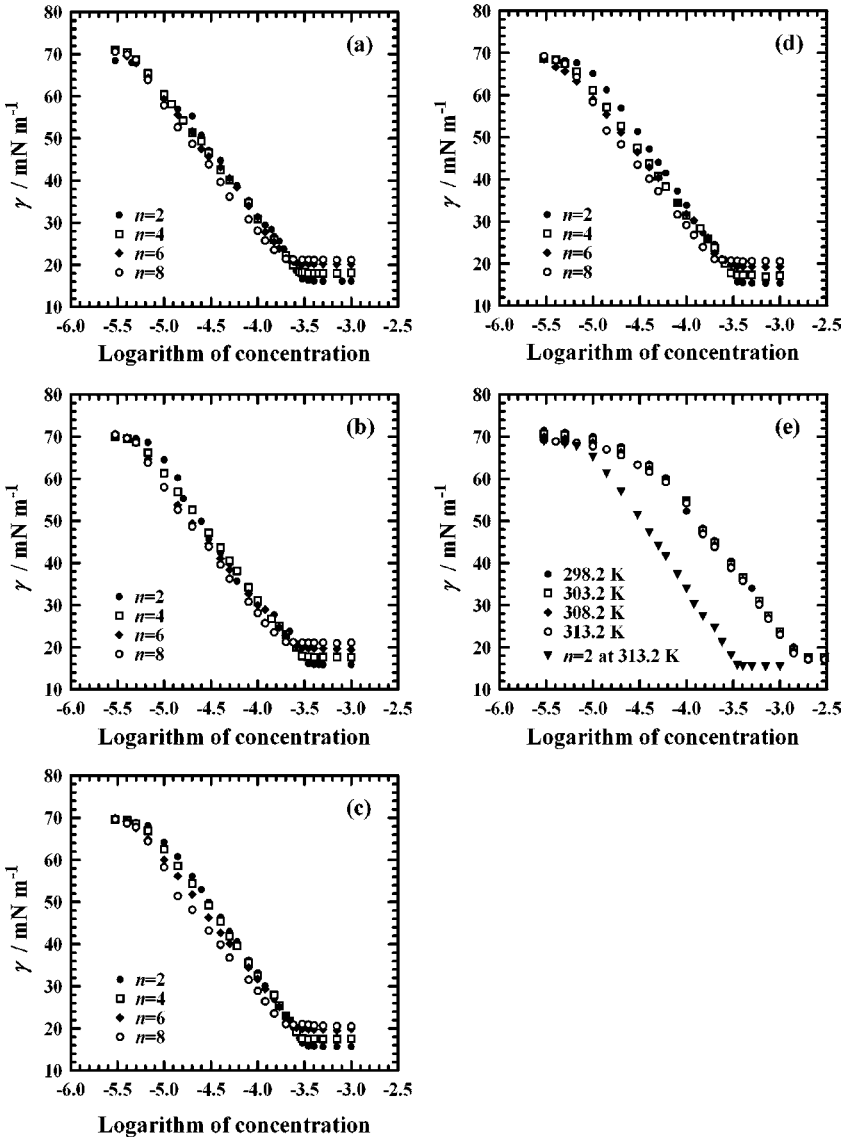

Figure 3. Changes of surface tension with logarithm of $C_nBP(FC_9)_2$ concentrations at (a) 298.2, (b) 303.2, (c) 308.2, and (d) 313.2 K; and with logarithm of $Mg(FC_9)_2$ concentrations within the same temperature ranges (e). The representative data of $n = 2$ at 313.2 K are also plotted in Figure 3(e).

Results and Discussion

Plots of surface tension (γ) against logarithm of concentration (C) for $C_nBP(FC_9)_2$ and $Mg(FC_9)_2$ at different temperatures from 298.2 to 313.2 K are shown in Figure 3, where similar changes are observed at each temperature. The γ values decrease with increase in concentration and then become constant (γ_{eq}) at higher concentrations, where the γ_{eq} values decrease with a decrease in charge separation (see Table 2). Although a big difference in surface tension cannot be seen among $C_nBP(FC_9)_2$ in Figure 3, the ability to reduce the surface tension at lower concentrations increased with increasing charge separation. These facts result from the difference in the molecular size among $C_nBP(FC_9)_2$.

Surface tension is sum of total interactions among molecules in surface region, and surfactant molecules are easy to concentrate in the surface region or in the vicinity of the air/water interface. Accordingly, the concentrated surfactant molecules can perturb and disorganize the three-dimensional (3-D) body of water molecules in the layer, leading to decrease in equilibrium surface tensions. A molecule of larger size can occupy a larger volume in the layer, inducing a high efficiency to reduce surface tension. It is quite noticeable that a linearity of surface tensions against the logarithm of concentration is retained over much a wider concentration range for $C_nBP(FC_9)_2$ than for conventional surfactants. This means that $C_nBP(FC_9)_2$ molecules disorganize the 3-D structure made of water molecules constantly over a wide concentration range, which is a quite unique characteristic of $C_nBP(FC_9)_2$. Moreover, considerable differences in the interfacial behavior can be seen between $C_nBP(FC_9)_2$ and $Mg(FC_9)_2$. $C_nBP(FC_9)_2$ are much more surface-active than $Mg(FC_9)_2$, although almost no difference in surface activity between $C_nBP(HC_{14})_2$ and $Cu(HC_{14})_2$ was observed as long as the charge separation is small.[9,10] It is suggested therefore that the spacers of ethylene groups are considerably important for surface behavior of the present fluorinated surfactants.

The critical micelle concentration (CMC) was determined as the concentration at an intersection of two straight lines through the points of surface tension below and above the CMC, which appears as a sharp break point in Figure 3. The obtained CMC values are listed in Table 2. The CMC values decrease with an increase in spacer length at each temperature, indicating that the longer-spacer hydrocarbon chain is more effective at facilitating the micelle formation. This is attributed to an increase in

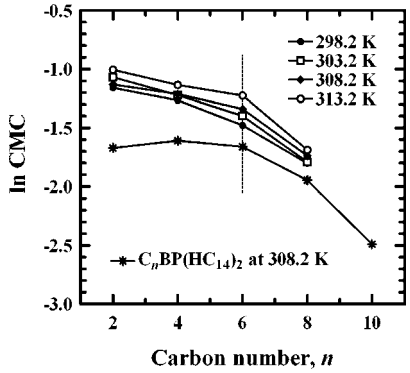

Figure 4. Dependence of ln CMC (mM unit) on the carbon number (n) of alkyl chains in $C_nBP(FC_9)_2$ at different temperatures and in $C_nBP(HC_{14})_2$ at 308.2 K.

hydrophobicity due to the extension of ethylene groups or inability to aggregate surfactant ions with its longer-spacer chain. A decrease in CMC has already been observed for univalent organic counterions.[14] Furthermore, the CMC slightly increased with increasing temperature over the temperature range 298.2−313.2 K (Table 2). This is due to an increase of molecular thermal motion. That is, the micelle formation of $C_nBP(FC_9)_2$ is more affected by the thermal motion than by hydrophobic dehydration. In addition, the CMC values of these surfactants were found to be larger than those of corresponding hydrocarbon analogues, $C_nBP(HC_{14})_2$,[10] where it is known as a rule that $C_nF_{2n+1}-$ corresponds to $C_{1.5n}H_{3n+1}-$ in hydrophobicity. Although it is widely accepted that a fluorinated surfactant has higher performance of micelle formation than a hydrocarbon surfactant, an unexpected result was obtained in the present study. Namely, the hydrocarbon spacer has a more positive contribution to micellization of hydrocarbon surfactants ($C_nBP(HC_{14})_2$) than fluorocarbon ones ($C_nBP(FC_9)_2$), inducing a relatively smaller CMC for $C_nBP(HC_{14})_2$. However, the CMC values of $C_nBP(FC_9)_2$ are smaller by 1 order of magnitude than those of the corresponding monomeric or dimeric surfactants with monovalent (Li^+, Na^+, K^+, and NH_4^+) and divalent (Mg^{2+}) charge-concentrated counterions.[12,15] The CMC values of these compounds are also listed in Table 2. From the above results, it can be said that ionic surfactants with charge-separated counterions have higher surface activity than conventional surfactants with charge-concentrated metallic ions.

Logarithms of the CMCs at each temperature are plotted against the carbon number of C_nBP spacer chain in Figure 4. Two different linear relationships below and above $n = 6$ are observed as is the case for the homologous hydrogenated surfactants, $C_nBP(HC_{14})_2$,[10] where the slopes for $n \leq 6$ are not treated in detail but are smaller in magnitude than those for $n \geq 6$. The free energy contribution ($\Delta G^\circ_{CH_2}$) of ethylene group in C_nBP spacers to the micelle formation can be calculated by the following equation

$$\Delta G^\circ_{CH_2} = -\left(1 + \frac{2}{\beta}\right) RT \frac{\Delta \ln \mathrm{CMC}}{\Delta n} \qquad (1)$$

where the degree of counterion binding to micelles ($\beta = 0.90$) is assumed at each temperature.[10] The free energy contributions per ethylene group thus obtained were estimated to be 0.4−0.7 kJ mol^{-1} from the slopes for $n \leq 6$ and 1.3−1.9 kJ mol^{-1} from those for $n \geq 6$ within the given temperature ranges, indicating that longer spacers have much larger contribution to the micelle formation. The above results also suggest that the counterion behavior around a micelle for $n = 8$ is different from that for $n \leq 6$. The free energy contribution of corresponding hydrocarbon surfactants ($C_nBP(HC_{14})_2$) was also evaluated in the previous paper.[10] The values were found to be ∼0 kJ mol^{-1} for $n \leq 6$ and 1.7 kJ mol^{-1} for $n > 6$ at 308.2 K. These free energy changes due to the extent of charge separation reasoned that alkanediyl chains of counterions fold and penetrate into the hydrophobic interior of the micelle just like the alkyl chain of a surfactant ion.[10] There exists a slight difference in the free energy contribution to the micelle formation between $C_nBP(FC_9)_2$ and $C_nBP(HC_{14})_2$. This might result from a complex interaction between fluorinated surfactant ions and hydrocarbon spacers. Such an interaction is discussed in more detail later.

The surface tension is a function of temperature, pressure, and chemical potential of components according to the Gibbs−Duhem equation for interface. As for a system of two phases (air and solution) and three components (surfactant, water, and air), the system becomes trivariant under the equilibrium state according to the phase rule. The following Gibbs equation is presented for the surface tension[16]

$$\mathrm{d}\gamma = -s^\mathrm{s}\,\mathrm{d}T + \tau^\mathrm{d}\,\mathrm{d}P - \Gamma\,\mathrm{d}\mu \qquad (2)$$

where s^s, τ^d, and Γ are the excess entropy per unit area at the interfacial layer, the thickness of the interfacial layer, and the surface excess of surfactant per unit area, respectively. At constant temperature and pressure, the surface excess of the surfactant becomes a function of the surfactant concentration

$$\Gamma = -\frac{1}{mRT}\left(\frac{\mathrm{d}\gamma}{\mathrm{d}\ln C}\right)_{T,P} \qquad (3)$$

where R is the gas constant, T is the absolute temperature, C is the surfactant concentration, and m is the number of chemical species per surfactant molecule whose concentration in the layer changes with the bulk concentration of the surfactant. For materials used in this study, the number of species (m) is three. The surface tension against the logarithm of the concentration CMC (Figure 3) was divided into two parts below and above the CMC, and the slope of the linear part below the CMC was used to determine the surface excess by eq 3.

The evaluated surface excess values for $C_nBP(FC_9)_2$ and $Mg(FC_9)_2$ are given in Table 3. The surface excess values of $C_nBP(FC_9)_2$ except for $n = 8$ decreased with increasing spacer length. However, the values for $n = 8$ and $Mg(FC_9)_2$ were different from expected ones. The former values resulted from the above-mentioned folding of spacer chain, and the latter ones are responsible for the large extent of hydration of magnesium ions. The Mg^{2+} hydration also induces the smaller surface tension (γ_{eq}) in comparison to similar monomeric surfactants,[12] which results from more destruction of the steric structure formed by water molecules in the surface layer. Furthermore, it can be roughly said that the surface excess of all surfactants listed in Table 3 decreased with increasing temperature due to an increase in thermal motion of the molecules.

From the surface excess, the apparent molecular surface area (A) in the surface layer can be calculated by

$$A = \frac{1}{N_\mathrm{A}\Gamma} \qquad (4)$$

(14) Hoffmann, H.; Platz, G.; Rehage, H.; Reizlein, K.; Ulbricht, W. *Makromol. Chem.* **1981**, *182*, 451−481.

(15) Hoffmann, H.: Ulbricht, W.; Taggesson, B. *Z. Phys. Chem.* **1979**, *113*, 17−36.

(16) Guggenheim, E. A. *Thermodynamics; An Advanced Treatment for Chemists and Physicists*, 6th ed.; Elsevier North-Holland Inc.: New York, 1977; pp 46−49.

Table 3. The Surface Excess (Γ), Apparent Molecular Surface Area (*A*), and pC_{20} of Each Compound at Different Temperatures

compound	temp. (K)	10^{-6} Γ (mol m^{-2})	*A* (Å^2)	pC_{20}
$C_2BP(FC_9)_2$	298.2	1.88	88	4.64
	303.2	1.82	91	4.68
	308.2	1.88	88	4.54
	313.2	1.81	92	4.46
$C_4BP(FC_9)_2$	298.2	1.71	97	4.72
	303.2	1.69	98	4.60
	308.2	1.79	93	4.59
	313.2	1.62	103	4.60
$C_6BP(FC_9)_2$	298.2	1.67	99	4.72
	303.2	1.57	105	4.77
	308.2	1.60	104	4.59
	313.2	1.50	110	4.60
$C_8BP(FC_9)_2$	298.2	1.77	94	4.77
	303.2	1.74	96	4.77
	308.2	1.68	99	4.74
	313.2	1.63	101	4.74
$Mg(FC_9)_2$	298.2	1.72	97	3.98
	303.2	1.70	97	3.90
	308.2	1.68	99	3.89
	313.2	1.66	100	3.91
$C_2BP(HC_{14})_2$[a]	308.2	1.69	98	–
$C_4BP(HC_{14})_2$[a]		1.64	101	–
$C_6BP(HC_{14})_2$[a]		1.50	111	–
$C_8BP(HC_{14})_2$[a]		1.40	118	–

[a] Refs 10 and 11.

where N_A is the Avogadro's number. The obtained apparent areas are also listed in Table 3. The apparent molecular area increased with increasing spacer length and with increasing temperature as is usually observed. The results can be explained very simply. An increase in charge separation by an increase in spacer length directly leads to the swelling of molecular area of surfactant ions. The smaller the molecular area is, the greater the concentration required to reach the CMC, or there results a greater decrease in surface tension above the CMC. This agrees with the results in Figure 3. Herein, the important finding is that the apparent molecular area of $n = 8$ is smaller than that of $n = 6$. This variation was not observed for the case of $C_nBP(HC_{14})_2$. Such small molecular area resulted from a specific change in conformation of the counterion similar to bola-form counterions.[17−19] This means that the alkanediyl chain takes a somewhat free conformation above a certain length of spacer chain ($n = 8$) and then comes to form a loop structure with opposite tails of surfactant ions because of the weak interaction between fluorocarbon (surfactant ions) and hydrocarbon (C_nBP spacers). As for $C_nBP(HC_{14})_2$, on the other hand, it was reported that the alkanediyl chain of counterion (at even $n = 8$) enlarged the molecular area due to separation among surfactant ions. This is also the case for micellization, where the alkanediyl chain penetrates into the hydrophobic core of the micelles, inducing loop formation inside the micelles.[10] This is attributed to the attractive interaction between hydrocarbons of surfactant ions and the C_nBP spacer. Such a difference between fluorocarbon−hydrocarbon and hydrocarbon−hydrocarbon interactions generates much different solution properties between $C_nBP(FC_9)_2$ and $C_nBP(HC_{14})_2$.

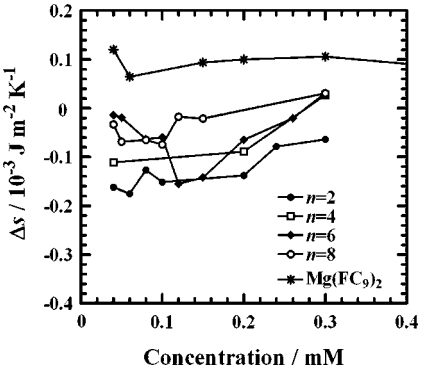

Figure 5. Entropy changes for surface adsorption or condensation with concentration of $C_nBP(FC_9)_2$ and $MgBP(FC_9)_2$ solutions over the whole temperature range studied.

The chemical potential of the surfactant is also a function of the temperature, pressure, and concentration

$$d\mu = -s\,dT + v\,dP + \left(\frac{d\mu}{dC}\right)_{T,P} dC \qquad (5)$$

where *s* and *v* are the partial molar entropy and volume, respectively. After introducing eq 5 into eq 2, the following equation is obtained

$$\Delta s = s^s - \Gamma s = -\left(\frac{d\gamma}{dT}\right)_{P,C} \qquad (6)$$

The Δ*s* values thus obtained are shown in Figure 5. In general, there exist two factors for contribution to the entropy change for surface adsorption: one is the positive contribution due to destruction of iceberg water molecules around hydrophobic chains, and the other is the negative contribution due to concentration of surfactant molecules. The entropy change of adsorption or surface condensation for $C_nBP(FC_9)_2$ roughly indicates negative values below the CMCs. This means that the concentration and the orientation of surfactant molecules in the interfacial layer accompanied by a negative entropy change contribute more to the total entropy change than the melting of iceberg water molecules around hydrophobic chain accompanied by a positive entropy change. As the spacer length increased, the entropy changes increased to zero below the CMCs. This can be reasoned by the fact that surfactants with a longer alkyl spacer are more difficult to concentrate or assemble. On the other hand, the changes for $Mg(FC_9)_2$ are positive at whole concentrations below the CMC, indicating that $Mg(FC_9)_2$ condensation toward the surface layer is substantially different in the condensed state from that of $C_nBP(FC_9)_2$. This fact also implies the importance of charge-separated counterions for surface activity of fluorinated ionic surfactants.

A convenient measure of the efficiency of surfactant adsorption or condensation into the surface region is the pC_{20} parameter introduced by Rosen,[20,21] which is a negative logarithm of the surfactant concentration required to reduce surface tension of solvent by 20 mN m^{-1}. As seen from Table 3, pC_{20} values increased with an increase in the spacer length. There is a large difference in the efficiency between $C_nBP(FC_9)_2$ and $Mg(FC_9)_2$. This difference means that fluorinated ionic surfactants with C_nBP^{2+} counterions have higher surface activity at smaller concentrations compared to those with Mg^{2+} counterions, supporting the importance of charge-separated counterions with in-between ethylene groups for the surface activity of fluorinated surfactants.

(17) Yiv, S.; Kale, K. M.; Lang, J.; Zana, R. *J. Phys. Chem.* **1976**, *80*, 2651−2655.
(18) Yiv, S.; Zana, R. *J. Colloid Interface Sci.* **1980**, *77*, 449−455.
(19) Zana, R.; Yiv, S.; Kale, K. M. *J. Colloid Interface Sci.* **1980**, *77*, 456−465.
(20) Rosen, M. J. *J. Am. Oil Chem. Soc.* **1974**, *51*, 461−465.
(21) Zhu, B. Y.; Rosen, M. J. *J. Colloid Interface Sci.* **1985**, *108*, 423−429.

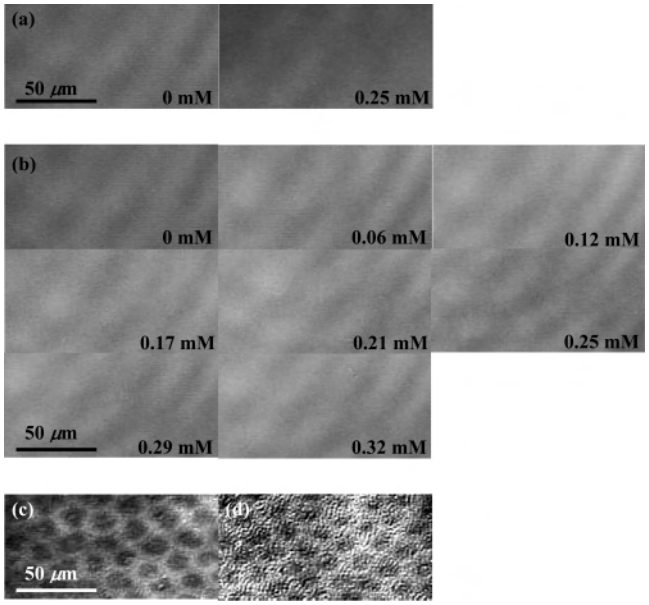

Figure 6. Representative BAM images of (a) $C_2BP(FC_9)_2$ and (b) $C_6BP(FC_9)_2$ at different concentrations at 298.2 K under the equilibrium state. BAM micrographs of insoluble monolayers of the analogous compounds [(c) $C_2BP(FC_{14})_2$ and (d) $C_6BP(FC_{14})_2$] on 0.15 M NaCl at 298.2 K at 12 mN m^{-1}, where ordered phases (dark) and disordered ones (bright) coexist.[26]

BAM images of the air/water interface for just water and two representative surfactant solutions ($n = 2$ and 6) at several concentrations below and above the CMCs are shown in Figure 6. If the emitted light is radiated to the water surface at the Brewster angle (53.1°), no reflected light is observed according to the theory. Therefore, a change in refractive index of water by condensation of surfactant molecules just at the air/solution interface brings about the reflection of the emitted light. If this is the case, some difference in contrast for the BAM image can be observed. However, all of the images for the present surfactant solutions were entirely the same as that of water alone. On the other hand, as for homologous insoluble surfactants ($C_2BP(FC_{14})_2$ and $C_6BP(FC_{14})_2$), which can form a stable Langmuir monolayer at the air/water interface, their ordered domains were clearly observed as dark islands in Figure 6. Even at the surface pressure which corresponds to the concentrations far below the CMC of $C_nBP(FC_9)_2$, a clear texture of the BAM image was observed for $C_2BP(FC_{14})_2$ and $C_6BP(FC_{14})_2$, because the insoluble surfactants truly locate at the air/water interface. No variation in BAM image of the present surfactant solutions might be the absence of the surfactant molecules just at the air/solution interface due to the image force for ionic species in water[22] or the condensation of surfactant ions at a certain distance below the interface.[13,23−25] In other words, these BAM images support at least the new concept of surface adsorption.[23,24]

Conclusions

The CMC and pC_{20} values are quite different between C_n-$BP(FC_9)_2$ and $Mg(FC_9)_2$, which means that the spacers of ethylene groups between pyridinium ions are considerably important for surface behavior of the present fluorinated surfactant ions. These differences were also confirmed by the entropy changes for surface adsorption or condensation. In addition, it was found that the extent of charge separation is related with their surface properties. Longer separation results in smaller CMC. By comparison of the results of $C_nBP(FC_9)_2$ with those of $C_nBP(HC_{14})_2$, the different folding modes were suggested for C_8BP spacers. The apparent molecular surface areas monotonically increased with an increase in spacer length for $C_nBP(HC_{14})_2$, whereas a small increase in the areas for $C_nBP(FC_9)_2$ was observed at $n \leq 6$. Furthermore, a spacer of the counterion for $C_nBP(HC_{14})_2$ folds and penetrates into the hydrophobic core of the micelle, whereas the spacer for $C_nBP(FC_9)_2$ is supposed to exist outside the micelle. This is attributed to a weaker interaction between fluorocarbon and hydrocarbon than between hydrocarbons themselves.

Acknowledgment. This work was supported by a Grant-in-Aid for Scientific Research 17310075 from the Japan Society for the Promotion of Science and by Grant 17650139 from the Ministry of Education, Science and Culture, Japan, and by Japan-Taiwan Joint Research Program which are gratefully acknowledged. This work (H.N.) was also supported by Research Fellowships of the Japan Society for the Promotion of Science for Young Scientists (18.9587).

LA7005474

(22) Korobeynikov, S. M.; Melekhov, A. V.; Furin, G. G.; Charalambakos, V. P.; Agoris, D. P. *J. Phys. D* **2002**, *35*, 1193−1196.
(23) Moroi, Y.; Rusdi, M.; Kubo, I. *J. Phys. Chem. B* **2004**, *108*, 6351−6358.
(24) Nakahara, H.; Shibata, O.; Moroi, Y. *Langmuir* **2005**, *21*, 9020−9022.
(25) Humphry-Baker, R.; Graetzel, M.; Moroi, Y. *Langmuir* **2006**, *22*, 11205−11207.
(26) Matsumoto, Y.; Nakahara, H.; Moroi, Y.; Shibata, O. *Langmuir*, accepted.